

## Growth of AlGaIn nanowires by metalorganic chemical vapor deposition

J. Su, M. Gherasimova, G. Cui, H. Tsukamoto, and J. Han<sup>a)</sup>

*Department of Electrical Engineering, Yale University, New Haven, Connecticut 06520*

T. Onuma, M. Kurimoto, and S. F. Chichibu

*Institute of Applied Physics, University of Tsukuba, Tsukuba 305-8573, Japan*

C. Broadbridge

*Department of Physics, Southern Connecticut State University, New Haven, Connecticut 06515*

Y. He and A. V. Nurmikko

*Division of Engineering, Brown University, Providence, Rhode Island 02192*

(Received 19 May 2005; accepted 12 September 2005; published online 27 October 2005)

Growth of ternary AlGaIn nanowires using metalorganic chemical vapor deposition is investigated. Structural, chemical, and optical characterization at nanoscopic scale is carried out by high resolution transmission electron microscopy, x-ray energy dispersive spectroscopy, and spatially resolved cathodoluminescence. Spontaneous formation of Al(Ga)N/GaN coaxial nanowires with distinct emission at 370 nm is observed. It is identified that the interplay between surface kinetics and thermodynamics facilitates the catalytic growth of GaN core while a limited surface diffusion of Al adatoms leads to nonselective, vapor-solid growth of Al(Ga)N sheath. The observation points to a fundamental difference in nanosynthesis using near-equilibrium and nonequilibrium techniques. © 2005 American Institute of Physics. [DOI: [10.1063/1.2126113](https://doi.org/10.1063/1.2126113)]

Catalytic growth based on the vapor-liquid-solid (VLS) principle<sup>1</sup> has attracted much attention recently as a self-directed procedure for creating semiconductor nanostructures. Homogeneous semiconductor nanowires<sup>2</sup> as well as axially modulated superlattices<sup>3</sup> have been reported. Synthesis of alloy nanowires with ternary and quaternary constituents is a stepping stone toward bandgap engineering in nanostructures. Few reports exist regarding the synthesis of alloy nanowires: AlGaAs nanowires were attempted by a solvothermal method,<sup>4</sup> molecular beam epitaxy (MBE),<sup>5</sup> and metalorganic chemical vapor deposition (MOCVD).<sup>6</sup> Choi *et al.*<sup>7</sup> observed phase segregation of in the synthesis of wide band gap AlGaIn nanowires using hot-wall chloride vapor epitaxy. Recently we demonstrated the synthesis of GaN nanowires by a cold-wall commercial MOCVD platform<sup>8</sup> employed in AlGaInN heteroepitaxy.<sup>9</sup> In this letter we report our investigation of nonequilibrium synthesis of AlGaIn nanowires as building blocks for nanowire heterostructures. It is discovered that spontaneous formation of coaxial AlGaIn nanowires occurs over most of the composition range (20%–90%). Morphological, structural, and optical characterization is carried out to elucidate the origin of observed spatial separation. A model based on competitive surface diffusion and interplay with thermodynamics is proposed self-consistently, illustrating both the flexibility and complexity in nanosynthesis using nonequilibrium growth techniques.

Synthesis of AlGaIn nanowires was carried out in a commercial horizontal MOCVD reactor (Aixtron 200/4 HT-S) with trimethylgallium (TMGa), trimethylaluminum (TMAI), and trimethylindium as the group III precursors and ammonia (NH<sub>3</sub>) as the group V source. The total flow of TMGa and TMAI is held constant<sup>10</sup> while the Al content in the vapor phase,  $x_{\text{Al-gas}} = [\text{TMAI}] / ([\text{TMAI}] + [\text{TMGa}])$ , is varied from 0% (GaN) to 100% (AlN). Polycrystalline alumina sub-

strates coated by Ni thin films (4–8 Å) are used as templates. Scanning electron microscopy (SEM) was performed using a FEI XL30 field-emission microscope. High-resolution transmission electron microscopy (TEM) and x-ray energy dispersive spectroscopy (EDS) was performed using a JEOL 2010 FasTEM microscope. Spatially integrated or resolved cathodoluminescence (CL) was excited by a cw electron(e) beam with or without the e-beam scanning within a modified JEOL JSM-880M, and dispersed by a 20 cm focal length grating monochromator equipped with a scanning electron microscope. Monochromatic spatially resolved CL images were taken at selective wavelengths at  $T = 105$  K.

The morphology of MOCVD-grown AlGaIn nanowires with varying vapor-phase Al content is surveyed by SEM and summarized in Fig. 1. Nanowires are observed in samples with Al vapor content from 30% to 90%. As the Al concentration is increased, an inverse dependence is observed between the length of nanowires and the density of nanowires/nanocrystals. Samples with a high  $x_{\text{Al-gas}}$  exhibit a clean background and a low density of long (4–5 μm) nanowires while samples with low  $x_{\text{Al-gas}}$  are characterized by short, rod-like (1–2 μm) nanowires with nanocrystals decorating the background. Growth of GaN in the absence of TMAI results in a high density of short nanorods and anisotropic nanocrystals [Fig. 1(a)] while growth of AlN leads to a thin film coating that conforms to the morphology of alumina substrates (large grains), as shown in Fig. 1(f).

Microstructural analysis was carried out on nanowires that had been sonicated in ethanol solution and dispersed onto TEM grids; a typical example is shown in Fig. 2(a). A contrast of the dark inner core and the light outer sheath is observed in all of the AlGaIn nanowires imaged. Thickness and degree of tapering of the outer sheath region increases with the increase of  $x_{\text{Al-gas}}$ ; a slope of ~11 nm/μm is estimated for the 90% sample (not shown). Chemical analysis by selective area EDS, with an electron-beam cross section

<sup>a)</sup>Electronic mail: [jung.han@yale.edu](mailto:jung.han@yale.edu)

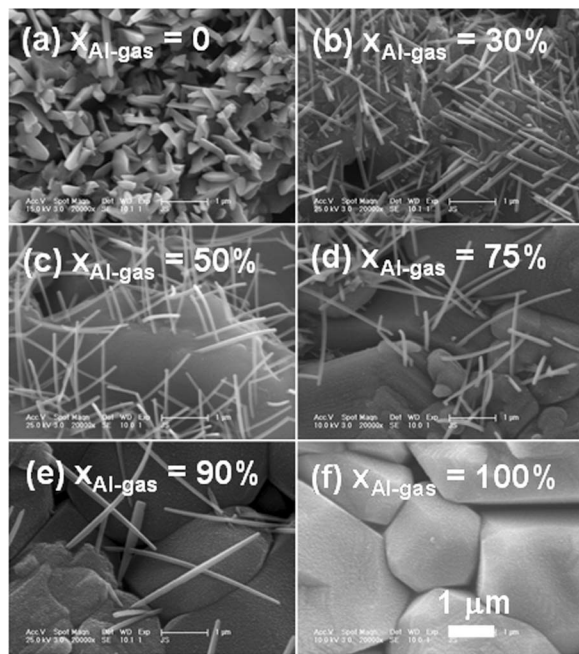


FIG. 1. SEM images of AlGaIn nanowires on alumina templates with Al phase ratio  $x_{\text{Al-gas}}$ =30%, 50%, 75%, and 90%.

of 3 nm in diameter, was performed at five different spots over the width of the nanowires [“+” in Fig. 2(a)]. A normalized composition profile is shown in Fig. 2(b). The chemical composition profile [Fig. 2(b)], which correlates well with the contrast in the TEM image [Fig. 2(a)], indicates the presence of an Al-rich sheath region and a core consisting of primarily GaN. Our observation of spontaneous formation of coaxial AlGaIn nanostructures agrees phenomenologically with the earlier finding<sup>7</sup> of synthesis of AlGaIn nanowires by the hot-wall chloride vapor reactor. It was proposed in Ref. 7 that the 2.4% lattice mismatched strain between AlN and GaN is the driving force responsible for the formation of spatially segregated coaxial nanowires.

Nanowire synthesis based on near-equilibrium VLS principle in flow-tube environment is a well-documented phenomenon.<sup>11</sup> Growth selectivity is derived from a preferential incorporation of vapor species through or around catalyst nanodroplets and a negligible growth rate elsewhere between the vapor and solid interface imposed by minuscule supersaturation near equilibrium. In the synthesis of nanowires using nonequilibrium, epitaxial techniques such as MOCVD and MBE, adatom kinetics including surface and gas phase diffusion need to be taken into consideration.<sup>12</sup> It was shown recently<sup>13</sup> with chemical beam epitaxy that growth of InAs nanowires takes place primarily through

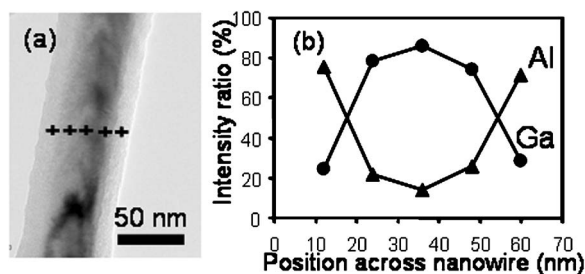


FIG. 2. (a) TEM of AlGaIn nanowires with  $x_{\text{Al-gas}} = 50\%$ . (b) Normalized composition profile across the nanowire.

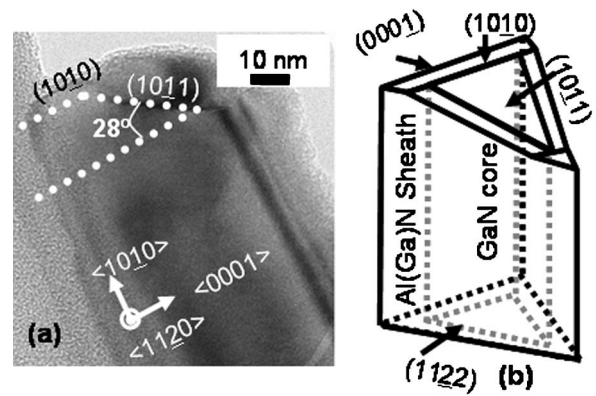


FIG. 3. (a) High-resolution TEM image of AlGaIn ( $x_{\text{Al-gas}} = 50\%$ ) nanowire near the tip region, the nanowire growth direction is along  $\langle 1010 \rangle$ , it is viewed along the  $\langle 1120 \rangle$  direction, with a very small degree of tilting toward  $\langle 0001 \rangle$  or  $\langle 000\bar{1} \rangle$  direction. (b) Three-dimensional diagram of the nanowire tip, the triangular cross section is bound by two  $\{1011\}$  planes and basal  $\langle 0001 \rangle$  plane, the droplet is on the tilted  $\langle 1011 \rangle$  plane.

mass transport of In adatoms within the radius of diffusion length and incorporation preferentially at catalyst tips. In nonequilibrium synthesis of AlGaIn nanowires by MOCVD, the presence of both Al and Ga adatoms as well a large difference in bond strength and consequently diffusion mobility<sup>14</sup> create a unique interplay between kinetic and thermodynamic processes.

Figure 3(a) shows a high-resolution TEM image near the tip of a nanowire with a growth direction along  $\langle 1010 \rangle$ . For all the nanowire tips examined, the width of the core (GaN) region, as determined by the light/dark contrast, is well correlated with the physical dimension of catalyst droplets, suggesting that the preferential incorporation into and the formation of GaN core region is linked to the catalytic growth. The presence of an Al-rich Al(Ga)N outer sheath that is located outside the shadow projection of nanodroplets is less likely to be attributed to catalytic growth. Separate studies of the lack of epitaxial lateral overgrowth (ELO) of AlGaIn (Ref. 15) and limited surface diffusion of Al adatoms tend to support a model that the AlGaIn outer sheath is formed through conventional vapor-solid growth with negligible selectivity. Such a designation provides an explanation of the increased tapering of AlGaIn nanowires with an increasing  $x_{\text{Al-gas}}$ , since the tapering slope represents an approximate measure of the radial and axial growths.<sup>16</sup> The dimensional agreement between catalyst nanodroplets and the core diameter of coaxial nanowires has also been observed in intentional overgrowth of InGaIn shell on catalytically grown GaN nanowires.<sup>17</sup>

High-resolution TEM reveals the presence of well-defined crystallographic planes at the nanowire tips [Fig. 3(a)]. Crystallographic analysis indicates that the inclined droplet/nanowire interface ( $62^\circ$  to growth direction) corresponds to a pyramidal  $\{1011\}$  plane, a plane likely to have the lowest surface energy or growth rate during MOCVD growth.<sup>18</sup> Based on the electron diffraction data, crystallographic symmetry consideration, and reported works of ELO, a three-dimensional rendition of the tip structure is given in Fig. 3(b). A well-known phenomenon in nanoscale nucleation, based on the Wulff theorem, is that a rapidly growing surface (or a facet with high surface energy) tends to grow itself out of existence. Our consideration of surface energetics [Fig. 3(b)], on the contrary, leads to an intriguing if not paradoxical distinction for nanowire growth in which

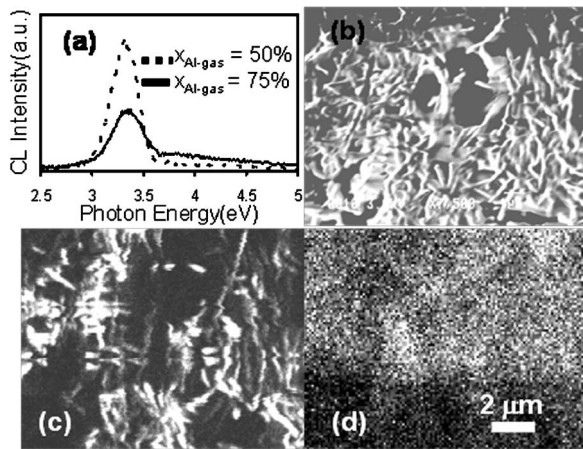


FIG. 4. (a) Wide area ( $10 \times 10 \mu\text{m}^2$ ) integrated scanning CL spectra at 105 K for AlGaIn nanowires with  $x_{\text{Al-gas}}=50\%$  and  $75\%$ , (b) SEM image of AlGaIn nanowires with  $x_{\text{Al-gas}}=75\%$  on alumina substrate, (c) monochromatic CL map of the same area at the wavelength of 370 nm (3.35 eV), and (d) monochromatic CL map of the same area at 320 nm (3.87 eV).

selective and preferential growth, mediated by the presence of catalyst and/or liquid droplets, takes place at and is confined to a surface/interface with a low surface energy,<sup>19</sup> thus affording a self-sustaining process for anisotropic growth.

To ascertain both optical quality and spatial distribution of the alloyed nanostructures, cathodoluminescence was performed on two samples with  $x_{\text{Al-gas}}=50\%$  and  $70\%$ . Figure 4(a) shows wide-area ( $10 \times 10 \mu\text{m}^2$ ) integrated scanning CL spectra in which emission from both samples are dominated by a GaN band-to-band recombination peak at 370 nm. A broad shoulder on the high-energy side ( $\sim 320$  nm) is also observed in both samples. The origin of different emission signatures is investigated through scanning CL mapping with monochromatic detection at wavelengths of 370 nm [Fig. 4(c)] and 320 nm [Fig. 4(d)]. A SEM image of nanowire morphology at the same location is recorded as a reference [Fig. 4(b)]. A match between the nanowire features under SEM [Fig. 4(b)] and the emission pattern at 370 nm [Fig. 4(c)] unambiguously associates the dominant GaN emission with individual nanowires, presumably from the core region. Furthermore, CL mapping at 320 nm reveals a nearly uniform distribution of AlGaIn, consistent with the notion that Al incorporates homogeneously without noticeable spatial selectivity.

Nonequilibrium techniques such as MOCVD and MBE have been instrumental in the growth of ternary and quaternary semiconductor heterostructures in planar epitaxy. Extension to nonplanar and/or patterned growth of alloys, however, often results in complex composition profiles due to competitive kinetics,<sup>20</sup> attested by our observation of spontaneous formation of coaxial AlGaIn nanowires under a supply of mixed vapor precursors in MOCVD process. As can be inferred from Fig. 1, in which an increase of  $x_{\text{Al-gas}}$  leads to a reduction in density and an increase in length of nanowires,

the surface diffusion of Ga adatoms is enhanced by the concurrent presence of Al adatoms, a phenomenon not readily observed in planar growth of AlGaIn alloys. This hypothesis is corroborated by a report that AlN is effective as an ELO mask,<sup>21</sup> indicating that the diffusion of Ga adatoms on AlN (or high Al containing alloy) is sufficiently enhanced for selective growth. We speculate that, during synthesis of AlGaIn nanowires by MOCVD, the passivation of the GaN core by the AlN sheath helps to stabilize the sidewall facets and improve nanowire yield at nucleation stage, bearing resemblance to earlier reports of control of surface energies using hydrogen<sup>19</sup> or oxygen<sup>22</sup> in nanoscale synthesis.

TEM assistance by A. Lehman and D. Ciuparu is acknowledged. This work at Yale is supported by the Department of Energy (DE-FC26-03NT41941) and the National Science Foundation (ECS-0304468).

<sup>1</sup>R. S. Wagner, in *Whisker Technology*, edited by A. P. Levitt (Wiley, New York, 1970).

<sup>2</sup>X. Duan and C. M. Lieber, *Adv. Mater.* (Weinheim, Ger.) **12**, 298 (2000).

<sup>3</sup>M. S. Gudiksen, L. J. Lauhon, J. Wang, D. C. Smith, and C. M. Lieber, *Nature* (London) **415**, 617 (2002); Y. Wu, R. Fan, and P. Yang, *Nano Lett.* **2**, 83 (2002).

<sup>4</sup>P. D. Markowitz, M. P. Zach, P. C. Gibbons, R. M. Penner, and W. E. Buhro, *J. Am. Chem. Soc.* **123**, 4502 (2001).

<sup>5</sup>Z. H. Wu, M. Sun, X. Y. Mei, and H. E. Ruda, *Appl. Phys. Lett.* **85**, 657 (2004).

<sup>6</sup>K. Tateno, H. Gotoh, and Y. Watanabe, *Appl. Phys. Lett.* **85**, 1808 (2004).

<sup>7</sup>H. Choi, J. C. Johnson, R. He, S. Lee, F. Kim, P. Pauzauskie, J. Goldberger, R. J. Saykally, and P. Yang, *J. Phys. Chem.* **107**, 8721 (2003).

<sup>8</sup>J. Su, G. Cui, M. Gherasimova, H. Tsukamoto, J. Han, D. Ciuparu, S. Lim, L. Pfefferle, Y. He, A. V. Nurmikko, C. Broadbridge, and A. Lehman, *Appl. Phys. Lett.* **86**, 013105 (2005).

<sup>9</sup>M. Gherasimova, J. Su, G. Cui, J. Han, H. Peng, E. Makarona, Y. He, Y.-K. Song, and A. V. Nurmikko, *Mater. Res. Soc. Symp. Proc.* **798**, Y1.8 (2004).

<sup>10</sup>The sum of TMAI and TMGa flows is  $9.4 \mu\text{mol}/\text{min}$ ,  $\text{NH}_3$  flow is  $0.90 \text{ mmol}/\text{min}$ . Reactor pressure and temperature are maintained at 50 mbar and  $900^\circ\text{C}$ , respectively.

<sup>11</sup>E. I. Givargizov, *J. Cryst. Growth* **31**, 20 (1975).

<sup>12</sup>M. Kasu and N. Kobayashi, *J. Cryst. Growth* **174**, 513 (1997).

<sup>13</sup>L. E. Jensen, M. T. Bjork, S. Jeppesen, A. I. Persson, B. J. Ohlsson, and L. Samuelson, *Nano Lett.* **4**, 1961 (2004).

<sup>14</sup>M. Gherasimova, G. Cui, Z. Ren, J. Su, X. Wang, J. Han, K. Higashimine, and N. Otsuka, *J. Appl. Phys.* **95**, 2921 (2004).

<sup>15</sup>T. Detchprohm, S. Sano, S. Mochizuki, S. Kamiyama, H. Amano, and I. Akasaki, *Phys. Status Solidi A* **188**, 799 (2001).

<sup>16</sup>Based on the assumption that the slope is proportional to the ratio between radial and axial growth rates, an enhancement of Ga incorporation on the order of 800 is estimated.

<sup>17</sup>F. Qian, Y. Li, S. Gradecak, D. Wang, C. Barrelet, and C. M. Lieber, *Nano Lett.* **4**, 1975 (2004).

<sup>18</sup>K. Hiramatsu, K. Nishiyama, A. Motogaito, H. Miyake, Y. Iyecika, and T. Maeda, *Phys. Status Solidi A* **176**, 535 (1999).

<sup>19</sup>Y. Wu, Y. Cui, L. Huynh, C. J. Barrelet, D. C. Bell, and C. M. Lieber, *Nano Lett.* **4**, 433 (2004).

<sup>20</sup>R. Notzel and K. H. Ploog, *J. Cryst. Growth* **227–228**, 8 (2001).

<sup>21</sup>S. Heikman, S. Keller, S. P. Denbars, U. K. Mishra, F. Bertram, and J. Christen, *Jpn. J. Appl. Phys., Part 1* **42**, 6276 (2003).

<sup>22</sup>W. S. Shi, Y. F. Zheng, N. Wang, C. S. Lee, and S. T. Lee, *Chem. Phys. Lett.* **345**, 377 (2001).

Applied Physics Letters is copyrighted by the American Institute of Physics (AIP).  
Redistribution of journal material is subject to the AIP online journal license and/or AIP  
copyright. For more information, see <http://ojps.aip.org/aplo/aplcr.jsp>